# Performance Comparison of Cables with Partial Transposition

Chiara Frittitta, Pierluigi Bruzzone, Hugues Bajas, Federica Demattè, Kamil Sedlak

***Abstract*—The need of full transposition of the current carrying elements (strands) in large cables is frequently retained as top design criterion for conductors operating in pulsed mode. However, when the transposition error, i.e. the inductance difference among the strands, is small and the inter-strand resistance is low, the criterion can be relaxed for a certain range of operating conditions.**

**In this work, two partly transposed cables made of 18 $Nb_3Sn$ strands and one copper core (cu+6+12) and 19 $Nb_3Sn$ strands (1+6+12) are assembled in a SULTAN sample and tested under various operating conditions. No significant performance difference is observed, i.e. the 19 strands cable has slightly higher current sharing temperature, $T_{cs}$, than the 18 strands cable, as predictable from the superconductor cross section. The inductance imbalance in the 1+6+12 cable does not lead to either instability or performance loss. The test results support the soundness of the conductor layout of EUROfusion DEMO, where the 19 strands assembly is used as the first cable stage of the react & wind conductor.**

***Index Terms*— Cable Transposition, Current Distribution, Fusion Magnets.**

## I. INTRODUCTION

THE issue of perfect transposition in superconducting cables for pulsed operation was debated for over 50 years [1-5]. In easy words, perfect (or "full") transposition of the strands in a cable is obtained when each strand takes periodically the position of all the other strands. In a more formal way, the inductance (sum of self-inductance and mutual inductance) of each current carrying element is identical in a fully transposed cable.

A lack of transposition leads to unbalanced current distribution under pulsed operation, i.e. when voltage is applied to the cable, the strands with lower inductance carry larger current and eventually hit the critical current when other strands carry lower current. The full transposition of the strands in a cable is regarded as a requirement, e.g. in the ITER conductor design criteria [6]. On the other hand, Turck suggested since the early discussion in 1974 [1], that "The transverse conductance associated with series resistance can help distribution for very slowly rising currents".

In fact, the literature offers several examples of non-transposed cables, which worked satisfactory, e.g. the T-7 tokamak [7], the OMEGA detector [8], the ETL conductors [9] and the SULTAN 12 T coil [10]. For cables designed for 50 Hz operation, where the current carrying elements must be insulated to limit the AC loss, the full transposition remains a strict requirement.

The react-and-wind prototype conductors by the Swiss Plasma Center (SPC) for the DEMO toroidal field coil, namely RW3 [11] and RW4 [12] have non-transposed sub-cables, made by 1+6+12 strands. In an earlier prototype, RW2 [13] the sub-cables were made by one central copper wire +6+12 strands. The test in SULTAN of RW3 showed severe instabilities (sudden, random transitions), which were never observed in RW2. To clarify if the different behavior of RW2 and RW3 is linked to the sub-cable layout, a SULTAN sample is assembled and tested where one of the conductors is the sub-cable with 1+6+12 strands as RW3 and the other conductor has a central copper core, i.e. a layout made of 1cu+6+12 strands, as in RW2, see Fig.1.

## II. CONDUCTOR ASSEMBLY

About 10 m of the sub-cable, procured for the SPC prototype conductor named RW3 [11], were used for the preparation of the two conductors. The diameter of the Cr plated $Nb_3Sn$ strand is 1.0 mm and the twist pitch of the sub-cable is 105 mm. Two

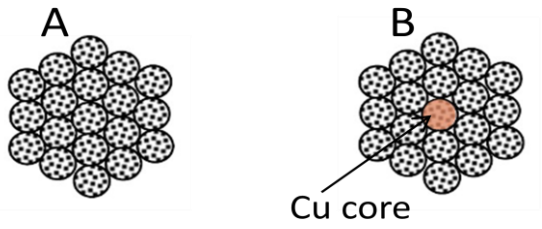


**Fig. 1.** The two conductors reproducing the layout of the sub-cables of RW3 (A, left) and RW2 (B, right).

Submitted for review September 19, 2023

This work has been carried out within the framework of the EUROfusion Consortium, via the Euratom Research and Training Programme (Grant Agreement No 101052200 — EUROfusion) and funded by the Swiss State Secretariat for Education, Research and Innovation (SERI). Views and opinions expressed are however those of the author(s) only and do not necessarily reflect those of the European Union, the European Commission, or SERI. Neither the European Union nor the European Commission nor SERI can be held responsible for them.

Chiara Frittitta, Pierluigi Bruzzone, Hugues Bajas, Federica Demattè and Kamil Sedlak are with EPFL-SPC, 5232 Villigen PSI, Switzerland (email: chiara.frittitta@psi.ch, pierluigi.bruzzone@psi.ch, hugues.bajas@psi.ch, federica.dematte@psi.ch, kamil.sedlak@psi.ch).

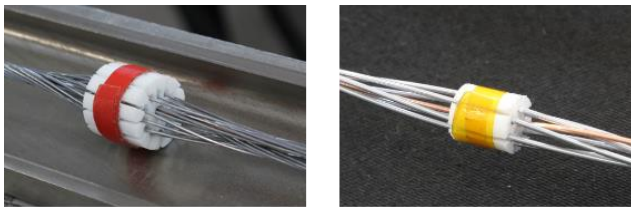

**Fig. 2.** Replacing the central strand by a copper wire.

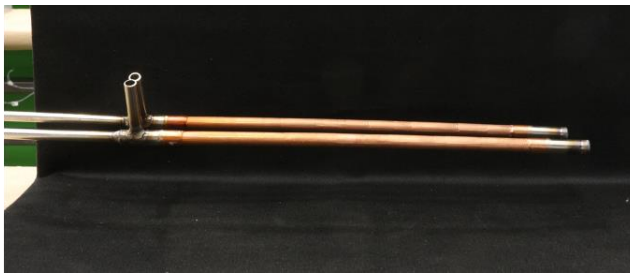

**Fig. 3.** The two conductors with steel jacket, copper termination and He inlet/outlet, before heat treatment.

sections of 3.5 m were cut and in one of the two cable bundles the central strand was replaced by a Cu strand. A plastic "ring" with slots was used to unwind the sub-cable, releasing the tension, replace the central strand by a copper wire of the same diameter and re-assemble the sub-cable. A bigger ring is used to unwind the external 12 strands (Fig. 2, left) and a smaller one is then used to unwind the inner crown of 6 strands (Fig. 2, right).

The two cable sections are then pulled through a 8 × 6 mm steel pipe and swaged to an inner diameter of ≈ 4.9 mm, giving a gentle compaction to the bundle. The cable length protruding on the ends of the steel pipe is cut to ≈ 255 mm.

The chrome is removed from the protruding ends of the cable, which are then fit into copper sleeves, acting as terminal, and compacted. A small Cu ring is applied to the ends of the cables before fitting it into the sleeves to avoid the unwinding of the cable. In Fig. 3 the position of the Helium inlet/outlet can be seen.

The two straight conductor sections are heat treated as in [11]. The conductor with 19 strands is named A and the one with 18 strands plus copper core is named B. The two small cable-in-conduit, CIC, are "wind-and-react", opposite to the large prototypes, RW3 [11] and RW2 [13], which are react-and-wind. A straight performance comparison is not possible due to the larger thermal strain in A and B compared to RW3.

After heat treatment the conductors A and B are assembled into a SULTAN sample with a soldered bottom joint. Temperature sensors and voltage taps are applied as in Fig.4. The even-numbered sensors are on conductor A, the odd-numbered ones on B. The voltage taps span four twist pitches (420 mm), centered in the high field zone of the sample.

## III. Analytical Discussion

In order to estimate the inductance imbalance due to the partial transposition, an analytical model was written making use of the formulas for two straight filaments placed in any desired position from [14]. For these calculations, the main input is the cable geometry; then the strands are divided into small elements along the lengths, which are used to compute the inductance matrix **M**. This analytical model allows investigating the inductance of a multi-strand cable with any twist pitch and strand configuration.

For clarification, some definitions are needed around the concept of inductance. The self-inductance $L$ is defined such that for a single strand the following equation is satisfied:

$$L\frac{dI}{dt} = V$$

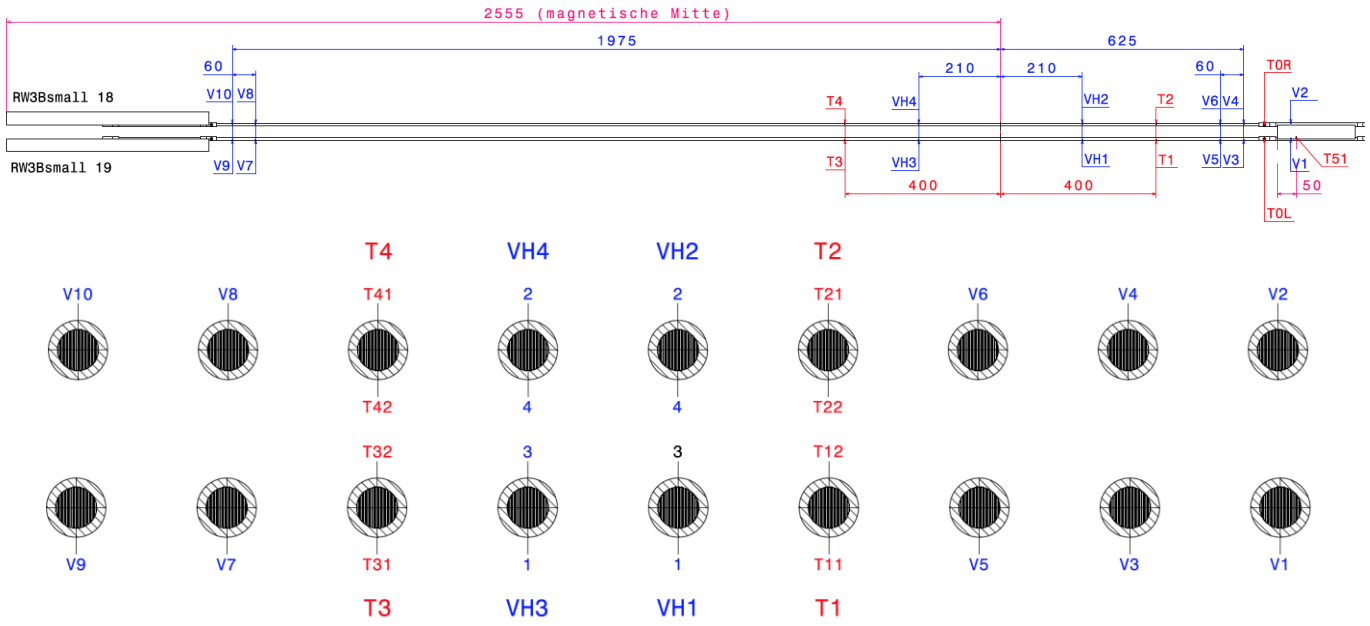


**Fig. 4.** Instrumentation of the SULTAN sample, with temperature sensors and voltage taps.

In a system consisting of several strands the inductance matrix **M**, composed by self and mutual inductances between strands, is used for the relation

$$\boldsymbol{M}\begin{pmatrix}\frac{dI_1}{dt}\\ \vdots \\ \frac{dI_n}{dt}\end{pmatrix}=\begin{pmatrix}V_1\\ \vdots \\ V_n\end{pmatrix}$$

where $\frac{dI_i}{dt}$ are the current ramps in each strand *i*. Lastly, the apparent self-inductance $\Lambda_k$ for a strand *k* is defined as

$$\Lambda_k \frac{dI_k}{dt} = V$$

where $\frac{dI_k}{dt}$ is the current variation on strand *k* in the case when all strands in parallel are subjected to the same voltage V:

$$\begin{pmatrix}\frac{dI_1}{dt}\\ \vdots \\ \frac{dI_n}{dt}\end{pmatrix}=\boldsymbol{M}^{-1}\begin{pmatrix}1\\ \vdots \\ 1\end{pmatrix}V.$$

The latter definition is the one used in the following, where the apparent self-inductance and the resulting current distribution for the presented cables is investigated. Fig. 5 shows the self-inductance of each strand calculated for a 0.5m long conductor like the one presented in this work (twisted) and for the case of infinite twist pitch (straight). The twist increases the self-inductance, but the same is not true for the apparent self-inductance $\Lambda_k$, as the weight of the mutual inductance dominates. This can be seen in the graph in Fig. 6 where the calculated $\Lambda_k$total inductance for each strand, in the case of $V = 1V$, is plotted for various twist pitches and for the straight case.

A comparison of the inductance behavior in Fig. 5 and Fig. 6 shows that while the self-inductance increases when the strands are twisted, the mutual inductance is highest in the case of the straight array. Therefore, it should be possible to find a so-called "perfect" twist pitch, for which the apparent self-inductance is balanced among the strands. To find such twist pitch an iterative minimum search was performed, which indicates that the "perfect" twist pitch, in the case of the 1+6+12 layout, is close to 13 mm for 1mm strands, see blue line in Fig. 6. However, this twist pitch is not realistic because for a cable with 4.9 mm diameter, the shortest practical twist pitch is 50-60 mm.

Considering now the tested conductor A, the limit case of insulated strands was investigated to predict the worst current limitation. In this case the current cannot redistribute between the strands and thus the conductor will quench when the strands with the smallest apparent self-inductance, and thus the largest current, will reach its critical current $I_c$. Using the apparent self-inductances reported in Fig. 6, the cable quench current for the insulated model is found, according to the scaling law, to be $I_q^{cable} = 0.77 I_c^{cable}$, which corresponds to a current degradation of 23%. Under the same assumptions, the quench current calculated for conductor B in case of full insulated strands is $I_q^{cable} = 0.81 I_c^{cable}$, corresponding to a current degradation of 19%.

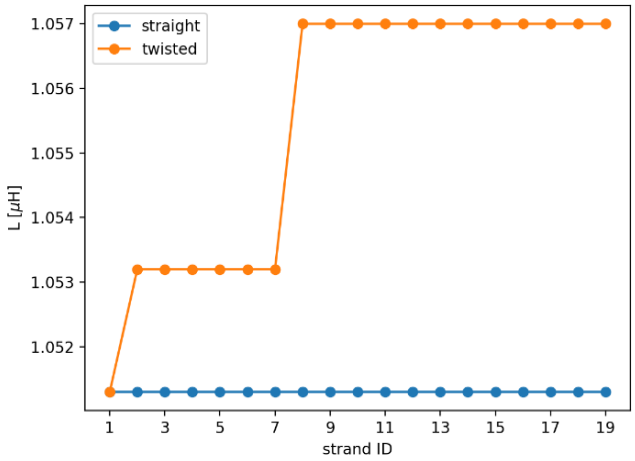


**Fig. 5.** Self-inductance of each strand in the case of twisted (105mm twist pitch) and untwisted configuration for a 0.5m long conductor. Here strand ID 1 corresponds to the central strand, 2-7 to the middle shell and 8-19 to the outer shell.

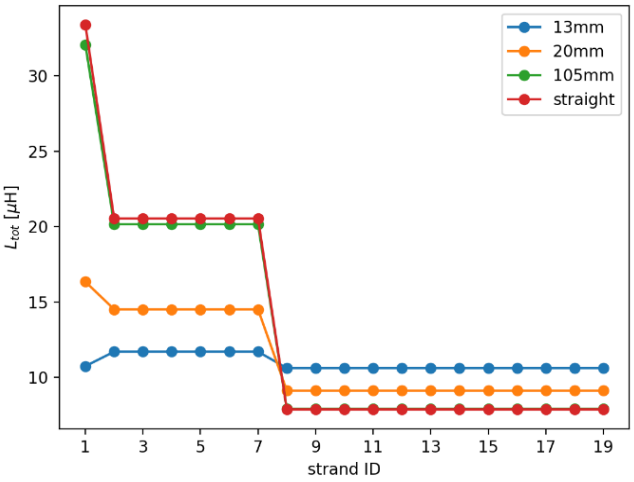


**Fig. 6.** Calculated apparent self-inductance of each strand for different twist pitches, including the "perfect" twist pitch of 13mm. The total length considered is 0.5m.

In order to investigate analytically realistic current profiles among the strands in the tested conductors, the electrical network model from [15] was used with Dirichlet boundary conditions (fixed current) as discussed in [16]. The input currents are the above defined $\frac{dI_k}{dt}$ normed to the total $\frac{dI}{dt}$ of the cable. For this analysis different scenarios were investigated with various values of inter-strand resistance. The conductor considered is conductor A, with a total length of 10 twist pitches.

For a linear inter-strand resistance of $10\Omega m$ (practically insulated strand) the model shows no current redistribution, as shown in Fig. 7. Next to the strands, the cable performance is indicated by the solid black line and the current limitation is highlighted by the dashed vertical line. For a more typical inter-

strand resistance, such as $1n\Omega$m, current redistribution takes place around $I_c$, see Fig. 8. When strands 8-19 (in the outer shell) exceed $I_c^{strand}$, the ohmic voltage drives the current re-distribution according to the inter-strand resistance.

For higher applied voltage, i.e. higher current rate, the ohmic voltage to drive the current re-distribution increases. For very high applied voltage, the ohmic voltage on strands 8-19 exceeds the take-off before current re-distribution is established.

## IV. Test Results

The test in SULTAN is focused on the DC performance by current sharing temperature, $T_{cs}$, test. The operating current is set at 4.7 kA to reproduce the same current density as in the RW3 conductor, i.e. 66 kA / 14 sub-cables [11]. The mass flow rate is set at ≈1 g/s in each conductor.

The $T_{cs}$ runs were carried out in the background field of 8 T to 11 T. The current was raised in steps, with 100 A/s. The take-off electric field is >100 µV/m. As the performance of A and B is very close, the $T_{cs}$ at 10 µV/m could be assessed in the same run for both conductors. The $T_{cs}$ for conductor A (19 strands) is systematically higher than conductor B. The highest difference, 90 mK, is at 10.9 T background field. A summary of the $T_{cs}$ results is shown in Fig. 9. The expected performance for A and B is also shown in Fig. 9 using the scaling law and assuming balanced current distribution and a longitudinal strain of -0.6%, typical for wind-and-react CIC.

The transient field stability was investigated in the background field of 9 T and operating current of 4.7 kA. A trapezoidal field was applied with ramp rate up to 2 T/s, amplitude 0.4 T and flat top duration of 10 s. The temperature increase by the transient field was of the order of 0.1 K (small AC loss) and no quench was observed.

## V. Conclusion

The test results of the two conductors, obtained with slow current and temperature ramp, prove that the performance scales with the number of strands, in good agreement with the prediction assuming -0.6% thermal strain, i.e. the low transverse resistance allows an effective re-distribution of the current, as discussed in section III. Both conductors are stable against transient field events up to 2 T/s. The instabilities observed in RW3 cannot be correlated with the sub-cable layout.

The calculation of the inductance shows that a short twist pitch mitigates the current unbalance in pulsed operation. For the tested conductors, with 105 mm twist pitch, the predicted performance would drop by ≈20% in case of insulated strands.

The lack of instability and the good match with the scaling law prediction suggest that for the operating range of the EUROfusion DEMO TF magnets, a cable layout with non-fully transposed first cable stage, either A or B type, is acceptable.

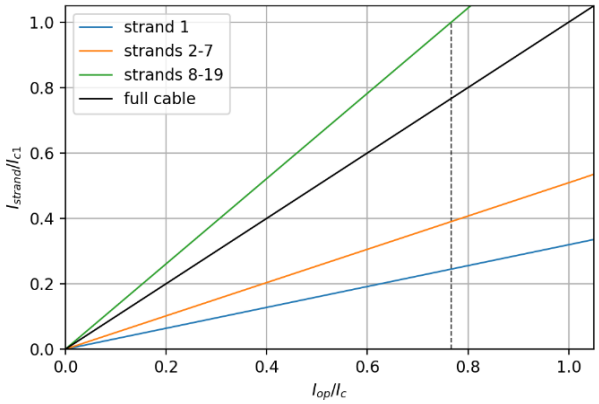


**Fig. 7.** Current profile for an inter-strand resistance of $10\Omega m$ (i.e. insulated strands), where no current redistribution is possible within physical limits. The black solid line represents the cable performance, while the dashed vertical line indicated the current limitation, i.e. when the outermost strands hit maximum current.

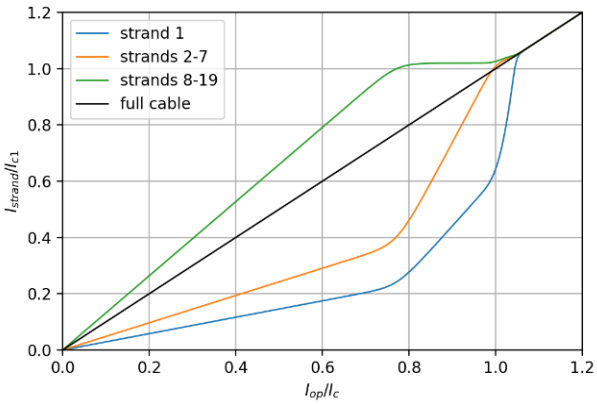


**Fig. 8.** Current profile for the conductor A with an inter-strand resistance of $1n\Omega m$. The current redistribution takes place close to $I_c$.

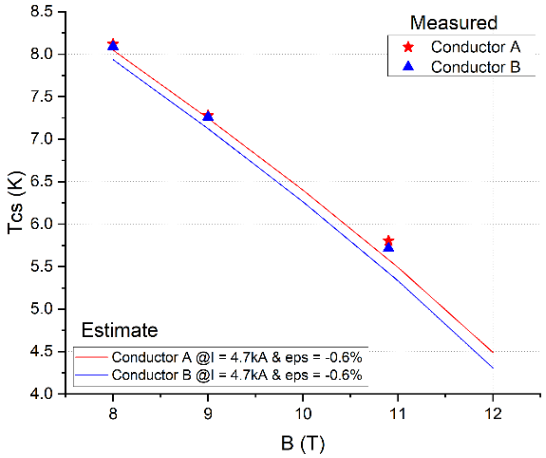


**Fig. 9.** Summary of $T_{cs}$ results, including also the expected values from the scaling law, assuming -0.6% long. strain. For A, the $T_{cs}$ is 8.09 K, 7.28 K and 5.77 K. For B, the $T_{cs}$ is 8.12 K, 7.26 K and 5.84 K at background field of 8 T, 9 T and 11 T respectively.

## ACKNOWLEDGMENT

The authors are indebted with the SPC workshop and SULTAN operation team for their skilled and dedicated support. The magic of Franz Oberle is specially appreciated, who managed replacing the central strand of the sub-cable by a copper wire.

Federica Demattè is in debt with Nikolay Bykovskiy for the continuous help with MATLAB and the many insights when discussing the results of the presented model.

## REFERENCES

[1] B. Turck, "Influence of a transverse conductance on current sharing in a two-layer superconducting cable." *Cryogenics* 14.8 (1974): 448-454.

[2] G. Ries, “Stability in superconducting multistrand cables”, *Cryogenics*, 20, 9, 513-519, 1980.

[3] L. Bottura, M. Breschi and M. Fabbri, "Analytical solution for the current distribution in multistrand superconducting cables", *Journal of Applied Physics* 92.12 (2002): 7571-7580.

[4] R. Kang *et al.*, "The current unbalance in stacked REBCO tapes--simulations based on a circuit grid model", *arXiv preprint arXiv:2302.06817* (2023).

[5] N Amemiya, “Overview of current distribution and re-distribution in superconducting cables and their influence on stability”, *Cryogenic*, 38, 5, 545=550, 1998.

[6] ITER Final Design Report 2001: DRG1 Annex “Magnet Superconducting and electrical Design Criteria”, IAEA Vienna 2001.

[7] D. P. Ivanov *et al.*, “Test results of “tokamak-7” superconducting magnet system (SMS) sections”, *IEEE Trans.Magn.* 15, 550, 1979.

[8] N. Schaetti, “Superconductors for the magnet coils of the Omega spark chamber at CERN”, *Brown Boveri Review* 59**,** 2/3, 73 (1972)

[9] K. Agatsuma *et al.,* “Braided multifilamentary $Nb_3Sn$ hollow superconductor and its magnet”, *IEEE Trans. Magn.* 15, 787 (1979)

[10] B. Jakob, G. Pasztor, “Fabrication of a high current $Nb_3Sn$ forced flow conductor for the 12 Tesla SULTAN test facility”, *IEEE Trans. Magn.* 23, 914 (1987)

[11] H. Bajas, Final Report of MAG-4.2-T012-D002, Dec. 2021, https://idm.euro-fusion.org/?uid=2NB9V9

[12] F. Demattè *et al*., "Preliminary Design of a High Current R&W TF Coil Conductor for the EU DEMO," *IEEE Trans. Appl. Supercond*, vol. 32, 4202504, 2022

[13] P. Bruzzone, K. Sedlak, B. Stepanov, M. Kumar and V. D'Auria, "A New Cabled Stabilizer for the $Nb_3Sn$ React&Wind DEMO Conductor Prototype," *IEEE Trans. Appl. Supercond*, vol. 31, 4802505, 2021.

[14] F. Grover, “Inductance Calculations – Working Formulas and Tables”, *Dover Publications, Inc.* , pp. 55-58, ISBN: 0-87664-557-0 (1946)

[15] N. Bykovskiy, “HTS high current cable for fusion application”, *PhD thesis EPFL*, https://infoscience.epfl.ch/record/231964

[16] L. Bottura, M. Breschi and A. Musso, “Calculation of interstrand coupling losses in superconducting Rutherford cables with a continuum model”, *Cryogenics*, 96 (2018) 44-52